Research Article

Cancer Immunology Research

Neoadjuvant Interferons: Critical for Effective PD-1–Based Immunotherapy in TNBC

Natasha K. Brockwell[1], Katie L. Owen[1], Damien Zanker[1], Alex Spurling[1], Jai Rautela[1], Hendrika M. Duivenvoorden[1], Nikola Baschuk[1], Franco Caramia[2], Sherene Loi[2,3], Phillip K. Darcy[2,3,4,5], Elgene Lim[6,7], and Belinda S. Parker[1]

Abstract

The lack of targeted therapies available for triple-negative breast cancer (TNBC) patients who fail to respond to first-line chemotherapy has sparked interest in immunotherapeutic approaches. However, trials utilizing checkpoint inhibitors targeting the PD-1/PD-L1 axis in TNBC have had underwhelming responses. Here, we investigated the interplay between type I IFN signaling and the PD-1/PD-L1 axis and tested the impact of combining IFN inducers, as immune activators, with anti–PD-1, to induce an antimetastatic immune response. Using models of TNBC, we demonstrated an interplay between type I IFN signaling and tumor cell PD-L1 expression that affected therapeutic response. The data revealed that the type I IFN-inducer poly(I:C) was an effective immune activator and anti-metastatic agent, functioning better than anti–PD-1, which was ineffective as a single agent. Poly(I:C) treatment induced PD-L1 expression on TNBC cells, and combined poly(I:C) and anti–PD-1 treatment prolonged metastasis-free survival in a neoadjuvant setting via the induction of a tumor-specific T-cell response. Use of this combination in a late treatment setting did not impact metastasis-free survival, indicating that timing was critical for immunotherapeutic benefit. Together, these data demonstrated anti–PD-1 as an ineffective single agent in preclinical models of TNBC. However, type I IFN inducers were effective immune activators, and neoadjuvant trials combining them with anti–PD-1 to induce a sustained antitumor immune response are warranted. *Cancer Immunol Res; 5(10); 871–84. ©2017 AACR.*

Downloaded from http://aacrjournals.org/cancerimmunolres/article-pdf/5/10/871/2351462/871.pdf by guest on 26 August 2022

Introduction

Immunotherapy has gained momentum as a viable option to treat a subset of cancers. Therapies targeting immune checkpoint proteins such as cytotoxic T-Lymphocyte antigen 4 (CTLA4) and the programmed death-1 (PD-1) receptor have revolutionized the treatment of metastatic melanoma (1, 2). The inhibitory action of PD-1 bound to its ligand (PD-L1) dampens immune activation—a mechanism exploited by tumor cells via upregulation of cell-surface PD-L1 expression to evade immune detection and subsequent tumor cell elimination (3, 4). Studies exploring the efficacy of treatments such as nivolumab and pembroluzimab, PD-1–specific antibodies, have demonstrated 1-year survival rates of over 73% in patients with metastatic melanoma, a vast improvement over post-chemotherapy survival (5, 6). Extended follow-up into the durable response of nivolumb reports a 5-year overall survival rate of 34%; this is more than double the previous survival rate for patients with metastatic melanoma receiving chemotherapy (7). Therefore, such agents are now being trialed in other cancer types, including breast cancer.

In breast cancer, use of anti–PD-1/PD-L1 has received most attention in the triple-negative breast cancer (TNBC) subtype. TNBC tumors have high PD-L1 expression compared with other subtypes (8, 9) and a high degree of tumor-infiltrating lymphocytes (TILs; ref. 10), suggesting that they may be more immunogenic (11). Additionally, due to the lack of targeted therapies available for this subtype, new approaches are urgently needed for patients who do not respond to first-line chemotherapy. Trials utilizing checkpoint inhibitors in metastatic TNBC patients are ongoing. Reported response rates are encouraging, albeit lower than those reported in melanoma. A phase 1b trial (NCT01848834) assessing the safety and efficacy of pembroluzimab in pretreated metastatic TNBC expressing PD-L1 reported a response rate of 18.5% in 27 patients, yet only 1 complete response and limited associated toxicities (12). In this pilot study, there was little correlation between the degree of PD-L1 positivity and clinical response. In fact, interrogation of PD-L1 expression in TNBC has revealed that high primary tumor PD-L1 expression predicts a favorable outcome (8, 9). Furthermore, PD-L1 expression directly correlates with the degree of TILs, which is another favorable prognostic factor (10, 13), suggesting that PD-L1 expression reflects an active antitumor immune microenvironment.

[1]Department of Biochemistry and Genetics, La Trobe Institute for Molecular Science, La Trobe University, Melbourne, Victoria, Australia. [2]Cancer Immunology Program, Peter MacCallum Cancer Centre, Parkville, Victoria, Australia. [3]Sir Peter MacCallum Department of Oncology, The University of Melbourne, Parkville, Victoria, Australia. [4]Department of Pathology, University of Melbourne, Parkville, Victoria, Australia. [5]Department of Immunology, Monash University, Clayton, Victoria, Australia. [6]Garvan Institute of Medical Research, Darlinghurst, Sydney, Australia. [7]St. Vincent's Hospital, University of New South Wales, Darlinghurst, Sydney, Australia.

Note: Supplementary data for this article are available at Cancer Immunology Research Online (http://cancerimmunolres.aacrjournals.org/).

Current address for J. Rautela: The Walter and Eliza Hall Institute of Medical Research, Parkville, Victoria, Australia; Department of Medical Biology, University of Melbourne, Victoria, Australia.

Corresponding Author: Belinda S. Parker, La Trobe Institute for Molecular Science, LIMS1, La Trobe University, Melbourne, VIC 3086, Australia. Phone: 61-3-9479-3020; E-mail: Belinda.Parker@latrobe.edu.au

doi: 10.1158/2326-6066.CIR-17-0150

©2017 American Association for Cancer Research.

These studies indicate that interactions between the immune system and breast cancer cells determine cell fate and risk of metastatic relapse in TNBC.

One family of cytokines implicated in an antitumor immune response are the type I interferons (IFNs; refs. 14, 15). We have shown the importance of tumor-intrinsic type I IFN signals in antitumor immunity and control of metastatic progression in breast cancer, whereby loss of tumor cell IFN regulatory factor (IRF) 7, a key transcription factor in the IFN signaling pathway, occurs in bone metastases in a syngeneic TNBC mouse model (16). Restoring tumor-cell IRF7 expression or systemic IFNα treatment could decrease bone metastasis and prolong survival, outcomes dependent on both innate and adaptive immune responses (16). In support of a metastasis-suppressive role of this pathway, loss of the IFN signature in primary breast tumors is associated with an increased risk of bone metastasis in patients (16). In multiple syngeneic TNBC mouse models, mice lacking the ability to respond to type I IFN signals [type I IFN receptor (IFNAR) deficient] are more susceptible to metastasis compared with wild-type mice (17). Furthermore, work in melanoma shows that IFN signaling is a tumor suppressive pathway; in particular, the downregulation of IFNAR1 contributes to aggressive metastatic melanoma (18). Together, this work implicates IFN-driven crosstalk between tumor cells and immune cells in the antitumor immune response during metastatic progression.

Type I IFNs have been used to treat melanoma (19), particularly in the adjuvant setting where such treatment prolongs disease-free survival in high-risk patients (20). However, type I IFN treatment has shown limited efficacy when tested in the context of advanced breast cancer (reviewed in ref. 14), possibly resulting from the lack of randomization within trials, coupled with treatment in late-stage treatment-refractory patients. Although few trials have explored the early treatment setting, several Toll-like receptor (TLR) agonists known to induce type I IFNs have demonstrated activity in early-stage breast cancer (14, 21). The combination of the TLR3 agonist poly(A:U) and chemotherapy (cyclophosphamide, methotrexate and 5-fluoro-uracil) or radiotherapy improved overall survival and 5-year relapse-free survival (14, 22). Despite this, the benefit of poly(A:U) or other IFN-based treatments as single agents or adjuvants to chemotherapy and radiotherapy has yet to be explored in early-stage TNBC trials.

Type I IFN-based treatments lead to upregulation of a multitude of IFN-stimulated genes (ISG) implicated in anticancer immune responses (14, 23, 24). This includes tumor-intrinsic changes (antigen presentation and stress ligand expression) and the activation of adaptive and innate immune components, such as $CD8^+$, $CD4^+$ T lymphocytes and natural killer (NK) cells (14, 15, 24), as well as promoting the secretion of IFNγ—a type II IFN that is cytotoxic (25, 26). However, an intrinsic brake on the IFN-based stimulation of immunity is the upregulation of immune checkpoints, including PD-L1 and PD-1 (27), which deactivate immune cells, largely to prevent autoimmunity (28). Such homeostatic strategies, however, could reduce the sustained impact of IFN-based therapeutic strategies. In line with this, therapeutic approaches combining immune activating agents with checkpoint blockade may be a viable immunotherapeutic strategy in patients.

This study investigates the utility of targeting type I IFN activation against, and in combination with, anti–PD-1 in both early and late treatment settings. As IFN-based immune activation can cause secondary dampening of immunity via PD-L1 induction (28), we hypothesized that PD-1 blockade would result in durable responses from immune activating therapies. We show that PD-1 blockade alone was ineffective as a single agent in several TNBC models regardless of treatment timing. We highlighted the anti-metastatic effect of targeting type I IFN activation via poly(I:C) administration and that its therapeutic benefit could be sustained via coadministration of anti–PD-1, particularly in the neoadjuvant treatment setting, and that this was associated with a sustained antitumor $CD8^+$ T-cell response.

Materials and Methods

Cell lines and mice

Human breast cancer cell lines were obtained from ATCC and DMSZ. TNBC cell lines were grown in DMEM supplemented with 10% FBS (Gibco; CAL-120, MDA-MB-231, SUM159, HCC70, BT20, and HCC1806) or RPMI supplemented with 10% FCS + 5 μg/mL insulin (Sigma; BT549, SUM149, MDA-MB-456), $HER2^+$ (HCC1954, SKBR3, MDA-MB-453), and ER^+ (BT483, T47D, MCF7) cell lines were also grown in 10% RPMI. Murine cell lines (67NR, 66cl4, 4TO7, and 4T1) were sourced from Dr. Fred Miller, who derived the cell lines from a spontaneous mammary tumor that arose in a BALB/c mouse (29). The highly metastatic 4T1.2 subclone of the 4T1 line was derived in and sourced from Prof. Robin Anderson's laboratory (30, 31). The EO771 cell line was derived from a spontaneous primary tumor in a C57BL/6 mouse and was kindly provided by Prof. Robin Anderson (32). All cells were engineered to express the mCherry and/or luciferase (Luc2) reporter genes through retroviral transduction (MSCV). BALB/c cell lines were cultured in α-MEM (5% FBS), and C57BL/6 cell lines were cultured in DMEM (10% FBS). All cell lines (human/murine) were passaged using EDTA (0.01% w/v in PBS) and cultured for no longer than 4 weeks. Tumor lines were verified to be *mycoplasma* negative by the Victorian Infectious Diseases References Lab at regular intervals and before *in vivo* injection of cell lines (Melbourne, Vic, Australia).

C57BL/6 and BALB/c mice were obtained from the Walter and Eliza Hall Institute of Medical Research (Melbourne, Vic, Australia) and the Animal Resources Centre (Perth, WA, Australia). Mice were used between the ages of 8 and 12 weeks. All experiments were approved by the La Trobe Animal Experimentation ethics committee.

Flow-cytometry analysis

Analysis of cell-surface PD-L1 expression *in vitro* and *in vivo* (circulating and infiltrating lymphocytes) was completed by flow cytometry using the FACS Canto II (BD Biosciences), and data were analyzed using FlowJo software (TreeStar). To assess PD-L1 induction by IFNα (250 IU/mL, 500 IU/mL, or 1000 IU/mL) and IFNγ (5 ng/mL, 10 ng/mL, and 20 ng/mL; Shendoah) cell lines were treated 48 hours prior to flow cytometry. Poly(I:C) (10 μg/mL) in the presence or absence of MAR1 (10 μg/mL; Life Technologies) was transfected into cells using lipofectamine 2000 (10 μg/mL, Life Technologies) 24 hours prior to flow cytometry. Cells were stained with CD274-PE (Human; 1:50, M1H5; Cell Signaling Technologies, Mouse; 1:300, M1H5; BD Biosciences), IFNAR1-APC (1:300, MAR1-5A3; Biolegend), or relevant isotype controls (Human; mouse IgG1 8; Cell Signaling Technologies, Mouse; rat IgG2a 8; Mouse IgG1 8 eBiosciences; Biolegend). Data are represented as normalized mean fluorescence intensity (MFI) where the median fluorescent intensity and standard deviation of

Downloaded from http://aacrjournals.org/cancerimmunolres/article-pdf/5/10/871/2351462/871.pdf by guest on 26 August 2022

the sample is normalized to the isotype control:

$$(\text{sample MFI} - \text{isotype MFI} / \text{sample robust SD} + \text{isotype robust SD})$$

Immune cell analysis

Blood obtained from the submandibular vein was used to profile circulating immune cells after red blood cell (RBC) lysis (155 mmol/L NH_4Cl, 10 mmol/L $KHCO_3$, 0.1 mmol/L EDTA, pH 7.3). Cells were stained with the following antibodies: CD8a-PE-Cy7 (53-6.7), CD4-APC-Cy7 (GK1.5), CD69-APC (H1.2F3), CD44-FITC (1M7), CD62L-BV421 (MEL-14), CD279-PE (J43), NK1.1-APC-Cy7 (PK136), NKP46-A700 (29A1.4), TCRβ-FITC (H57-597), CD11b-BV421 (M1/70), CD27-PerCP (LG-7F9; all from BD Biosciences), and NKG2D-PE-Cy7 (CX5; eBioscience) before being subjected to flow cytometry analysis.

Analysis of tumor-infiltrating lymphocytes was as above with the addition of mechanical and enzymatic [1 mg/mL collagenase I (Sigma) and 30 μg/mL DNAse I (Sigma) at 37°C] digestion to obtain a single-cell suspension before RBC lysis.

Intracellular cytokine staining (ICS) for IFNγ

To assess the number of antigen (Ag) specific $CD8^+$ T cells present in the lungs of mice, a single-cell suspension was obtained using mechanical and enzymatic [1 mg/mL collagenase I (Sigma) and 30 μg/mL DNAse I (Sigma) at 37°C] digestion before RBC lysis (155 mmol/L NH_4Cl, 10 mmol/L $KHCO_3$, 0.1 mmol/L EDTA, pH 7.3). Cell suspension was then restimulated with 4T1.2 cells for 5 hours in the presence of brefeldin A (BFA; 10 μg/mL, Sigma) before staining with CD8α-APC (53-6.7; BD Biosciences) followed by IFNγ-PE (XMG1.2; BD Biosciences) in the presence of saponin (0.4% v/v; as previously described by Zanker and colleagues, ref. 33). Samples were then subjected to flow cytometry using the FACSCanto II (BD Biosciences), and data were analyzed using FlowJo software (TreeStar).

Bioinformatic interrogation of breast cancer TCGA gene expression data

The TCGA Human Breast Invasive Carcinoma normalized RNA quantities were accessed using the Firehose platform (34). The IFN (16, 35) and IFN core (HBEGF, STAT1, IRF7, IFI44, IL13RA1, CD86, CSF2RB, CD44, TLR3, IER3, IFITM3, RUNX3, and CTSS) signatures were compared with PDL1 (CD274) expression. Pearson correlation coefficients (r), scatter plots, and significance values were computed in R (version 3.3.2).

In vivo treatment and metastasis analysis

For *in vivo* experiments, 1×10^5 cells (EO771 or 4T1.2) were resuspended in PBS and injected into the fourth mammary fat pad (IMFP) in a 20 μL volume on day 0. Poly(I:C) (25 μg/mouse; Sigma) or saline was administered intravenously (i.v.), whereas anti–PD-1 (RPM1-14, Bioxcell) IgG (2A3, Bioxcell) was administered intraperitoneally (i.p.) at 250 μg/mouse. To evaluate the effect of poly(I:C) on immune cell activation in 4T1.2 tumor–bearing mice, poly(I:C) was administered thrice weekly from days 2 to 11 after tumor cell inoculation.

Mice receiving the combined treatment strategy (treatment before and after primary tumor resection) were randomized into groups and administered poly(I:C) on days 6, 8, 11, 13, 15, and 18 and anti–PD-1 on days 8, 11, 15, and 18.

For the late treatment setting, after primary tumor removal, mice received poly(I:C) on days 13, 15, 18, 20, 22, and 25, and anti–PD-1 on days 15, 18, 22, and 25.

For the neoadjuvant treatment setting, mice received poly(I:C) on days 2, 4, 6, 9, and 11, and anti–PD-1 on days 4, 6, 9, and 11.

Mammary tumors were resected on day 12 (BALB/C) or day 15 (C57BL/6) after tumor cell inoculation and weighed. Mice were sacrificed upon signs of metastatic distress with all mice being taken at the same time point for metastasis assays. At end point, mice were imaged using an IVIS Lumina XR-III (Caliper Life Sciences, Australia) under inhaled isoflurane anesthesia before lungs were rapidly excised and subjected to *ex vivo* imaging. mCherry fluorescence or bioluminescent intensity (12 minutes post-i.p. injection of 1.5 mg D-Luciferin; Gold technology) was measured and normalized between all images in a group using Living Image 4.4 software (Caliper Life Sciences). Metastatic burden was assessed using quantitative real-time PCR as described below. Survival curves were generated using Prism (GraphPad).

Quantification of metastatic burden

Real-time (RT) qPCR was used to quantify metastatic burden (as previously described by Eckhardt and colleagues, ref. 36) by comparing the ratio of mCherry (present in tumor cells) to vimentin (NC_000068, present in all cells) sequences in genomic DNA preparations from homogenized and proteinase K (100 μg/mL, Merck) digested lungs and spines. PCR reactions were performed using SsoAdvanced universal probes supermix reagents (BioRad) and C100 Thermal Cycler with CFX96/CFX384 RealTime System module (BioRad) and primers were as follows: mCherry FWD: 5′-GACCACCTACAAGGCCAAGAAG-3′; REV: 5′-AGGTGATGTCCAACTTGATGTTGA-3′; hydrolysis probe: 5′/56-FAM/CAGCTGCCC/ZEN/GGCGCCTACA/3IABkFQ/3′: mVimentin FWD: 5′- AGCTGCTAACTACCAGGACACTATTG-3′; REV: 5′-CGAAGGTGACGAGCCATCTC-3′; hydrolysis probe: 5′HEX/CTTTCATGTTTTGGATCTCATCCTGCAGG/TAMRA/3′. Metastatic burden (arbitrary units; AU) was based on the quantification cycle (C_q) for mCherry relative to vimentin and displayed as relative tumor burden (RTB) using the following equation:

$$RTB = 10000/\left(2^{\Delta Cq}\right), \text{ where, } \Delta Cq = Cq(targetgene) - Cq(control)$$

Histology and immunohistochemistry (IHC)

Prior to paraffin embedding and sectioning, all tissues were fixed in 10% neutral-buffered formalin for 24 hours. For detection of PD-L1 expression, tissues were subjected to heat-induced epitope pressure cooker retrieval (110°C for 5 minutes) in EDTA buffer (1 mmol/L EDTA, pH 8) before incubating with anti–PD-L1 (AF1019; 1 μg/mL, R&D Biosystems) at 4°C overnight. Tissues were then incubated with enzyme-conjugated secondary antibody followed by incubation with Avidin/Biotinylated enzyme Complex (ABC; Vectastain) and visualization with the diaminobenzidine (DAB; Vectastain) color development system. Tissues were counterstained using hematoxylin.

Statistical analysis

Student two-tailed t tests were used to evaluate significant differences between groups. Mantel–Cox log-rank tests were used to evaluate differences in survival time. GraphPad Prism software (GraphPad) was used for all analyses. $P < 0.05$ was considered statistically significant.

Results

IFNs induced PD-L1 expression in TNBC primary tumors

To determine the heterogeneity of PD-L1 expression, we first assessed differences in cell-surface PD-L1 expression using flow

Downloaded from http://aacrjournals.org/cancerimmunolres/article-pdf/5/10/871/2351462/871.pdf by guest on 26 August 2022

cytometry across a range of cell lines, representing different subtypes. Of the cell lines evaluated, the TNBC subtype expressed the highest baseline PD-L1 expression (Fig. 1A). $HER2^+$ (ER^-/PR^-/HER2 amplified) and ER^+ cell lines expressed varying levels of PD-L1; however, ER^+ cells demonstrated the lowest expression (Fig. 1A). Although this pattern was concordant with PD-L1 expression in patient tissue cohorts (8, 9), expression was variable within our cell lines (Fig. 1A). As PD-L1 is an ISG and is induced in tumor cells by IFNγ (37), we assessed the impact of IFNα and IFNγ on cell-surface expression of PD-L1 in breast cancer cells. After a 48-hour incubation, IFNα and IFNγ treatment induced PD-L1 cell-surface expression in a range of human breast cancer cell lines (Fig. 1B).

The cell line work suggested a correlation between IFN signaling and PD-L1 expression. To test whether such a correlation exists in patient-derived breast tumors, we utilized the TCGA RNAseq database to compare the expression of our previously identified type I IFN gene signature (16, 35) and PD-L1. We identified a correlation between the IFN signature and also a core list we have developed that represents an active signaling pathway (HBEGF, STAT1, IRF7, IFI44, IL13RA1, CD86, CSF2RB, CD44, TLR3, IER3, IFITM3, RUNX3, CTSS) and PD-L1 expression (Fig. 1C and D). A link between therapeutic IFN induction and PD-L1 expression in

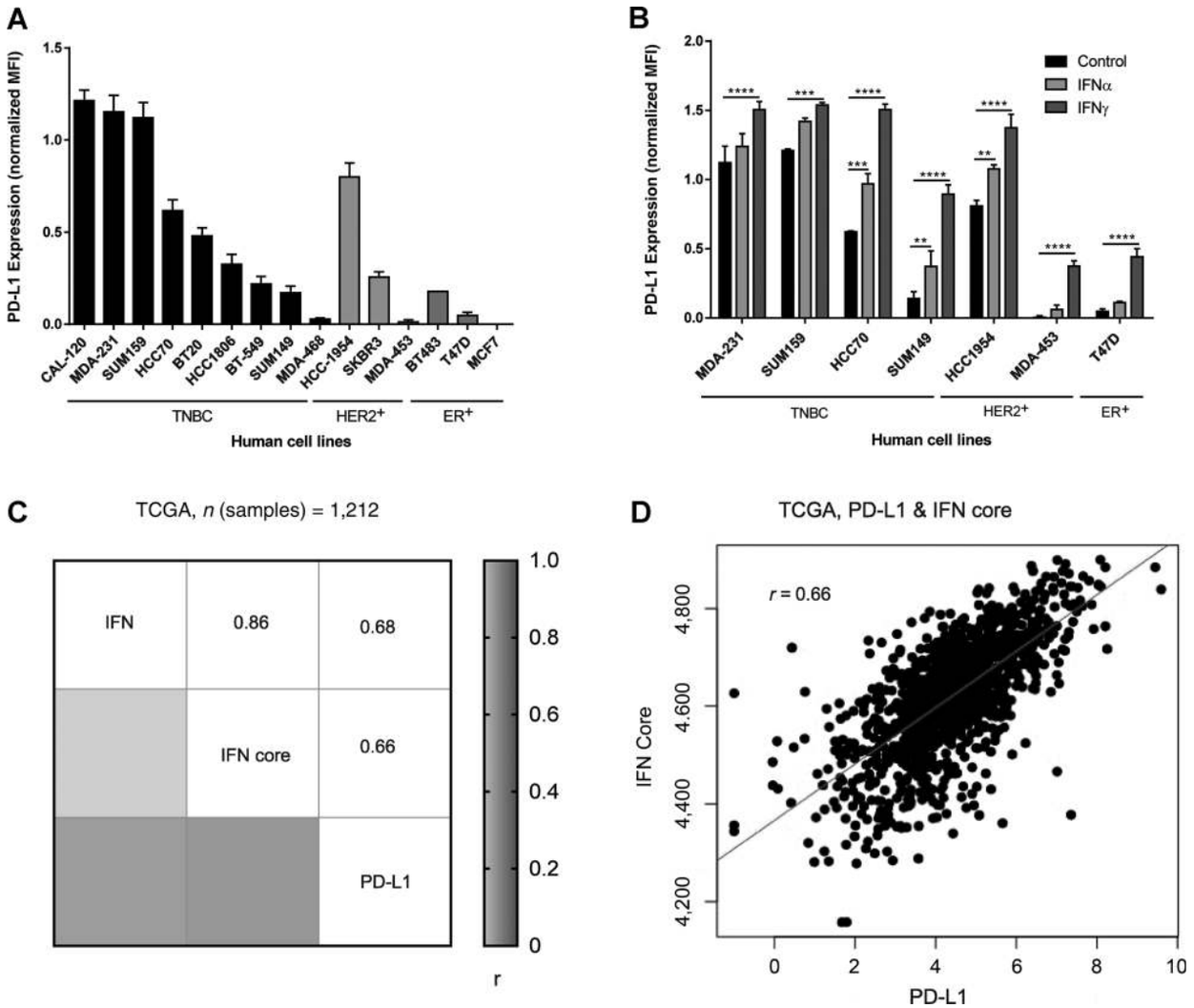

Figure 1.

Enhanced IFN signaling correlates with increases in PD-L1 expression in TNBC. Cell-surface PD-L1 expression determined by flow cytometry after staining with PE-conjugated anti–PD-L1 (M1H5) or isotype control (2A3). PD-L1 expression was measured in untreated cells (**A**) or cells treated with IFNα (**B**; 1,000 IU/mL) or IFNγ (10 ng/mL) for 48 hours prior to flow cytometry. FACS data are represented as normalized mean fluorescence intensity (MFI). $n = 3$; error bars, SEM; **, $P < 0.01$; ***, $P < 0.001$; ****, $P < 0.0001$ using Student t test. **C,** Correlation table representing the correlation of PD-L1 RNA expression with an IFN core list (also shown as a scatter plot in **D**) or full IFN signature in primary breast tumors ($n = 1{,}212$) from the TCGA RNAseq database. Pearson correlation coefficients (r) are indicated. All P values are $P < 0.0001$.

Downloaded from http://aacrjournals.org/cancerimmunores/article-pdf/5/10/871/2351462/871.pdf by guest on 26 August 2022

patients is yet to be tested, although our results support a link between an active type I IFN state and PD-L1 in TNBC patients.

IFN and IFN agonists increase PD-L1 expression both *in vitro* and *in vivo*

As with the human cells lines, mouse lines exhibited heterogeneous baseline PD-L1 cell-surface expression. The BALB/C series of cell lines (derived from a syngeneic TNBC mouse model) are well characterized for their metastatic propensity (29, 31). We observed that PD-L1 expression was higher in the nonmetastatic 67NR and weakly metastatic 66cl4 cell lines than in the highly metastatic 4T1 and 4T1.2 cell lines (Fig. 2A). The inverse correlation between PD-L1 expression and risk of metastasis is consistent with reports in TNBC patient tissues (8, 9). Regardless of baseline PD-L1 expression, both IFNα and IFNγ induced PD-L1 expression, up to 8- and 17-fold, respectively (Fig. 2A). Varying

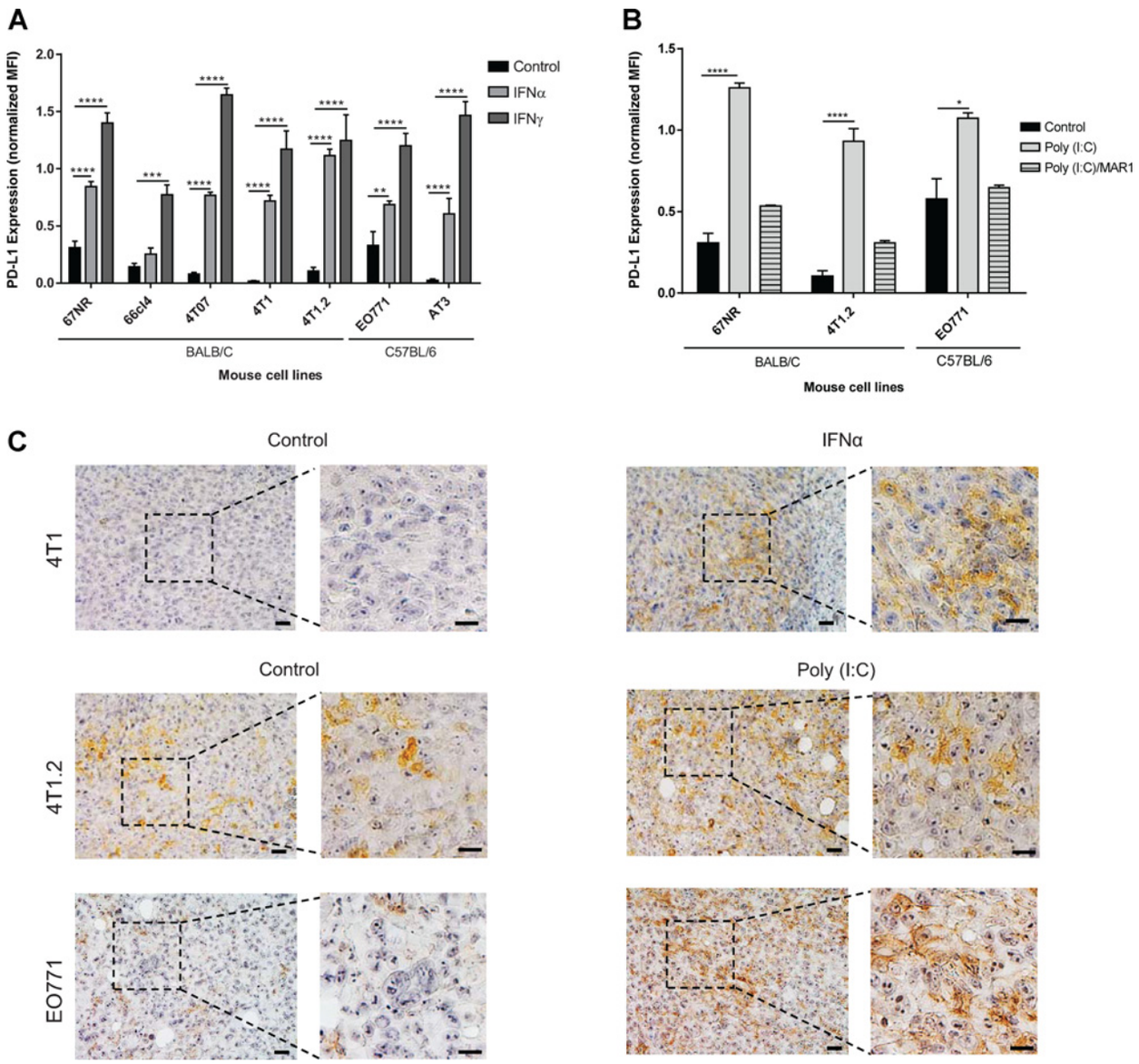

Figure 2.

IFN and type I IFN agonists increase PD-L1 expression in murine breast cancer cells *in vitro* and *in vivo*. Cell-surface PD-L1 expression determined by flow cytometry after staining with PE-conjugated anti–PD-L1 (M1H5) or isotype (2A3). Cells were treated *in vitro* with IFNα (1,000 IU/mL) or IFNγ (10 ng/mL) for 48 hours (**A**) or transfected with poly(I:C) (10 μg/mL) ± MAR1 (10 μg/mL) for 24 hours (**B**) as indicated before PD-L1 expression was measured by flow cytometry ($n = 3$). Error bars represent SEM. *, $P < 0.05$; **, $P < 0.01$; ***, $P < 0.001$; ****, $P < 0.0001$ using Student t tests. **C,** Immunohistochemical staining of PD-L1 expression in 4T1, 4T1.2, or E0771 primary tumors derived from mice that received IFNα (10^5 IU, i.p., thrice weekly), poly(I:C) (25 μg, i.v., thrice weekly) or saline (as indicated) prior to primary tumor resection. Tissues were stained using goat anti–PD-L1 (1 μg/mL) and PD-L1 expression visualized using DAB prior to nuclear counter-staining with hematoxylin. Representative pictures were taken of stained slides ($n = 5$ mice per group). Scale bars, 50 μm.

Downloaded from http://aacrjournals.org/cancerimmunolres/article-pdf/5/10/871/2351462/871.pdf by guest on 26 August 2022

doses of IFN revealed a dose-dependent increase in PD-L1 expression (Supplementary Fig. S1A and S1B). As TLR agonists that stimulate IFN production are being trialed clinically, we wanted to test whether the TLR3 agonist poly(I:C) also increased PD-L1 expression. Transfection of cells with poly(I:C) for 24 hours significantly upregulated cell-surface PD-L1 expression ($P > 0.05$). Addition of MAR1, a type I IFNα receptor (IFNAR) blocking antibody, abrogated poly(I:C) induced PD-L1 upregulation (Fig. 2B), confirming that poly(I:C) is stimulating PD-L1 expression via type I IFN production/signaling. This finding was independent of intrinsic IFNAR expression, with no differences detected between all cell lines evaluated (Supplementary Fig. S1C). Next, we evaluated expression of PD-L1 in orthotopic 4T1 mammary tumors derived from mice that had either received recombinant IFNα or a vehicle control. Our results demonstrate an increase in intratumoural expression of PD-L1 in mice treated with IFNα compared with untreated (Fig. 2C, no detectable expression in control to moderate expression in 50% to 60% cells in treatment group). Similarly, there was an increase in the number of PD-L1–positive tumor cells and higher staining intensity in the 4T1.2 (30%, moderate intensity in control to 70% moderate–high intensity with treatment) and E0771 (5% low intensity to >70% high intensity staining) tumors of mice treated with poly(I:C) (Fig. 2C). These results were concordant with our *in vitro* analysis. Taken together, these data demonstrate that tumor cell PD-L1 expression can be induced by IFN and support the hypothesis that PD-L1 is a marker of elevated immune signaling.

We also characterized the expression of activation ligands and PD-1 on the surface of circulating immune cells in tumor-bearing mice treated with poly(I:C). As expected, poly(I:C) led to enhanced $CD4^+$ and $CD8^+$ T- and NK-cell activation as indicated by the increase in activation ligands (CD69/NKG2D; Supplementary Fig. S2A and S2B). Further analysis of the NK cells revealed an increase in $CD27^{+/-}CD11b^+$ expression (Supplementary Fig. S2C). $CD27^+CD11b^+$ NK cells have an enhanced ability to secrete cytokines, and $CD27^-CD11b^+$ NK cells have efficient cytolytic function (38). Our results suggest that poly(I:C) treatment may enhance NK-cell activation and effector function, consistent with the known action of IFNs on immune activation. Both T and NK cells express PD-1, with poly(I:C) further increasing this expression, an effect more pronounced on NK cells (Supplementary Fig. S2D). Together, this suggested responses to poly(I:C) treatment could be improved if treatment also included anti–PD-1 to block the tumor cell PD-L1 interaction with cytotoxic T-cell or NK-cell PD-1 to further enhance an antitumor immune response.

Poly(I:C) and anti–PD-1 combination treatment slowed tumor growth and metastases

The EO771-mCherry syngeneic model was used to assess the impact of poly(I:C) and/or anti–PD-1 on primary tumor growth. Cells were injected intra mammary fat pad (IMFP) and mice received a priming dose of poly(I:C), followed by the combination of poly(I:C) and anti–PD-1 or single agent therapy (Fig. 3A). Analysis of primary tumor weight on day 15 after tumor cell inoculation revealed that combination therapy reduced tumor weight, whereas single agents alone did not affect primary tumor size compared with control (Fig. 3B). At day 15 post-primary tumor resection, mCherry tumor cells were visualized by *ex vivo* fluorescence imaging, and a reduction in lung metastatic burden was evident in the combination therapy group. Quantification of mCherry fluorescence revealed that both poly(I:C) alone and in combination with anti–PD-1 decreased lung metastasis (Fig. 3C and D). Such an impact was not observed in the anti–PD-1 treatment group that received anti–PD-1 alone.

Analysis of circulating immune cells during treatment confirmed an increase in the proportion of T cells expressing CD69 in the combination treatment group (Supplementary Fig. S3A). Furthermore, analysis of the $CD8^+$ T cells revealed an increase in the percentage of $CD44^+CD62L^+$ populations on day 14 in response to the combination treatment (Supplementary Fig. S3). Evidence suggests that $CD44^+CD62L^+$ $CD8^+$ T cells are representative of a central memory population (39), suggesting that poly(I:C) both alone and in combination with anti–PD-1 can increase the central memory population.

Poly(I:C) and anti–PD-1 combination treatment increases tumor-specific T-cell response

In order to assess the impact of combination therapy in a more aggressive model, we used the highly metastatic 4T1.2-luc2 cell line. Cells were injected IMFP into BALB/C mice and treatment initiated when tumors were palpable (day 6; Fig. 4A). Analysis of primary tumor weight on day 12 post-inoculation revealed that the combination therapy significantly decreased primary tumor weight compared with single agents alone ($P > 0.05$; Fig. 4B). Ten days after primary tumor resection, bioluminescence was used to detect 4T1.2 lung metastases *in vivo* and *ex vivo*. Bioluminescence was visibly decreased in the combination therapy group, indicating a reduction in overall metastatic burden (Fig. 4C), specifically in the lung (Fig. 4D). Quantitative DNA analysis of resected organs confirmed that combination treatment reduced metastatic burden in the lungs (Fig. 4E) of these mice compared with single agent and control-treated mice. Analysis of the lymphocyte population in the lungs of these mice revealed that the combination therapy significantly increased the number of tumor cell-specific IFNγ-producing $CD8^+$ T cells compared with poly(I:C) ($P > 0.05$; Fig. 4F and G). This increase in $CD8^+$ T-cell activity offers some rationale into the effectiveness of combining poly(I:C) and anti–PD-1 therapy.

Combination therapy was more effective in a neoadjuvant treatment setting

Having shown that the combination therapy was successful in this model, we wanted to test its impact in treatment settings relevant to the clinical context, mimicking either an early neoadjuvant setting before the detection of overt metastases or a late treatment setting whereby treatment commenced after primary tumor resection when metastases are detectable.

For the early neoadjuvant treatment setting, treatment commenced on day 2 and was ceased prior to primary tumor resection (Fig. 5A). Analysis of primary tumor weight revealed that poly (I:C) treatment reduced primary tumor weight compared with vehicle control and anti–PD-1 therapy groups (Fig. 5B), and the effect was more pronounced with combination therapy (Fig. 5B). Anti–PD-1 treatment alone had no effect on primary tumor weight. Analysis of tumor-infiltrating lymphocytes revealed that both single agents and combination therapy increased the total number of TILs (Fig. 5C). However, when we assessed the nature of these TILs, we found that only poly(I:C) treatment increased the percentage of $CD8^+$ and $CD4^+$ T cells expressing CD69 (Fig. 5D). Both poly(I:C) and the combination therapy increased the percentage of NK cells expressing CD69/NKG2D, suggesting an

Downloaded from http://aacrjournals.org/cancerimmunolres/article-pdf/5/10/871/2351462/871.pdf by guest on 26 August 2022

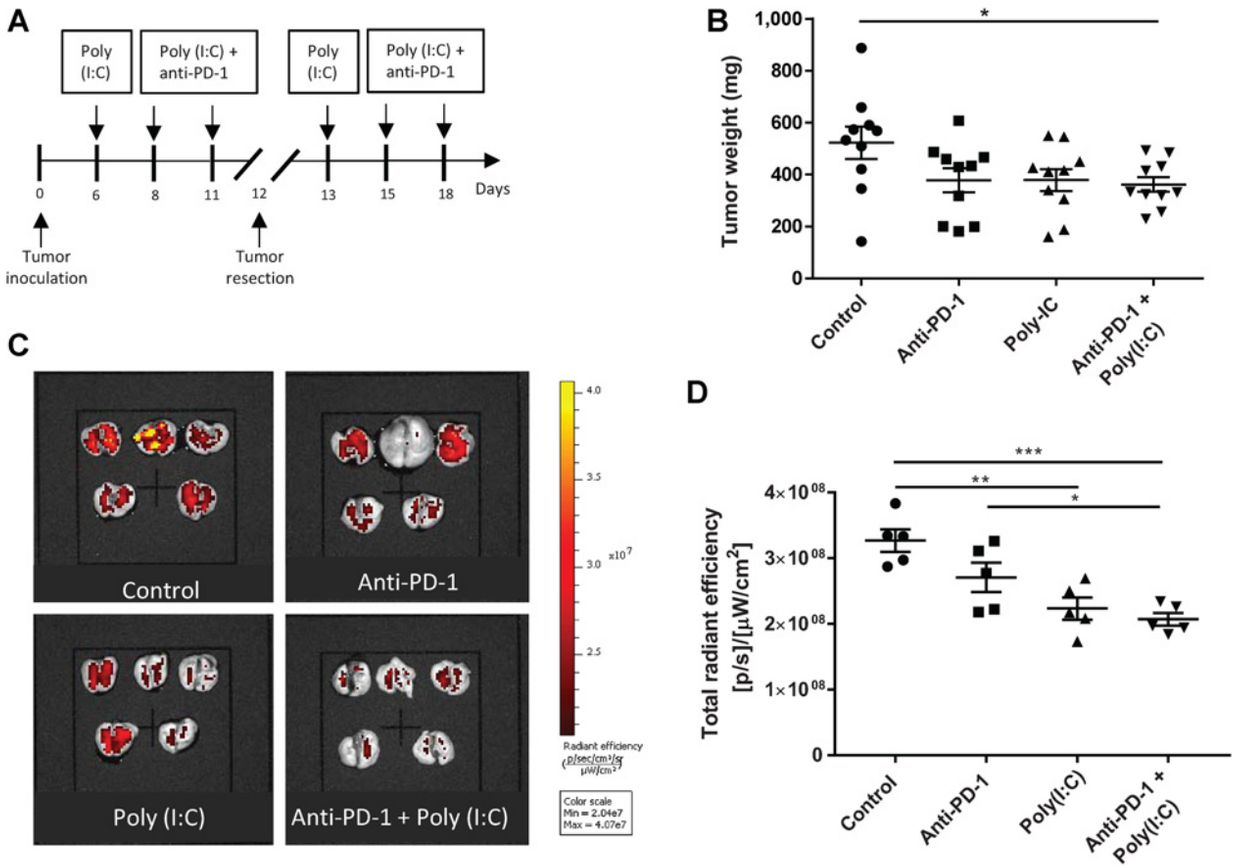

Figure 3.

Antibody-mediated PD-1 blockade in combination with poly(I:C) reduces primary tumor weight. **A,** Experimental protocol indicating timing of therapy in C57BL/6 mice inoculated IMFP with 1×10^5 EO771 cells and treated with poly(I:C) (25 µg, i.v.) and anti–PD-1 (RPM1-14; 250 µg, i.p.). **B,** Tumor weight (mg) 15 days post tumor cell inoculation ($n = 10$ per group). **C,** Representative mCherry fluorescent imaging of *ex vivo* lungs collected from EO771 tumor–bearing mice 30 days after tumor cell inoculation (of 5 mice representative of larger cohort). **D,** Total radiant efficiency of mCherry fluorescent lungs calculated using Living Image software (Lumina; $n = 5$ mice per group). Error bars represent SEM. *, $P < 0.05$; **, $P < 0.01$; ***, $P < 0.001$ using Student *t* tests.

increase in the activation status of immune cells infiltrating the primary tumor (Fig. 5E). During treatment, we also assessed circulating immune cells where we detected an increase in the percentage of $CD69^+$ and $CD27^{+/-}CD11b^+$ expressing NK cells in the poly(I:C) and the combination groups on day 10 (Fig. 5F). Thus, poly(I:C) not only increased TIL activation but also circulating immune cells, the latter of which likely combats metastatic spread.

We next assessed the impact of therapy on metastatic burden. Bioluminescent imaging of the thoracic cavity 11 days post tumor-resection (experimental end point) revealed reduced lung metastasis in poly(I:C) and combination treated mice (Fig. 6A and B). RT-qPCR analysis revealed that, again, anti–PD-1 therapy alone had no impact on lung metastasis and that both poly(I:C) and the combination therapy abrogated metastatic burden in the lungs in the neoadjuvant setting (Fig. 6C). Analysis of immune populations in the lung revealed that only combination therapy induced $IFN\gamma^+$ $CD8^+$ T cells (Fig. 6D and E), suggesting that the addition of anti–PD-1 to poly(I:C) therapy was required to induce a sustained T-cell antitumor response and that this could prolong metastasis-free survival. To test, this we performed metastasis-free survival studies, mimicking the neoadjuvant setting with mice being individually monitored for evidence of metastasis (Fig. 7A). Poly(I:C) single-agent therapy prolonged metastasis-free survival compared with control, yet anti–PD-1 alone had no impact on survival (median survival, 30, 25, and 24 days, respectively; Fig. 7B). Combination therapy significantly extended overall survival in this aggressive model (median survival, 38 days; Fig. 7B, $P > 0.05$) compared with single agents alone, supporting the combination of poly(I:C) and anti–PD-1 for prolonged antitumor immune response.

Such a survival benefit was not observed in a late treatment setting, in the absence of a primary tumor. We again used the highly metastatic 4T1.2-luc cells, which were injected IMFP, and treatment was initiated after primary tumor resection (Fig. 7C). Comparison of survival between treatment groups revealed that neither single agents or combination therapies had an impact on metastasis-free survival, with a median survival of 23 to 24 days for all groups (Fig. 7D). This was in stark contrast to the observed impact of such therapies in the neoadjuvant setting, suggesting that immune-mediated elimination of tumor cells was not effective against overt metastases in the absence of a primary tumor.

Downloaded from http://aacrjournals.org/cancerimmunolres/article-pdf/5/10/871/2351462/871.pdf by guest on 26 August 2022

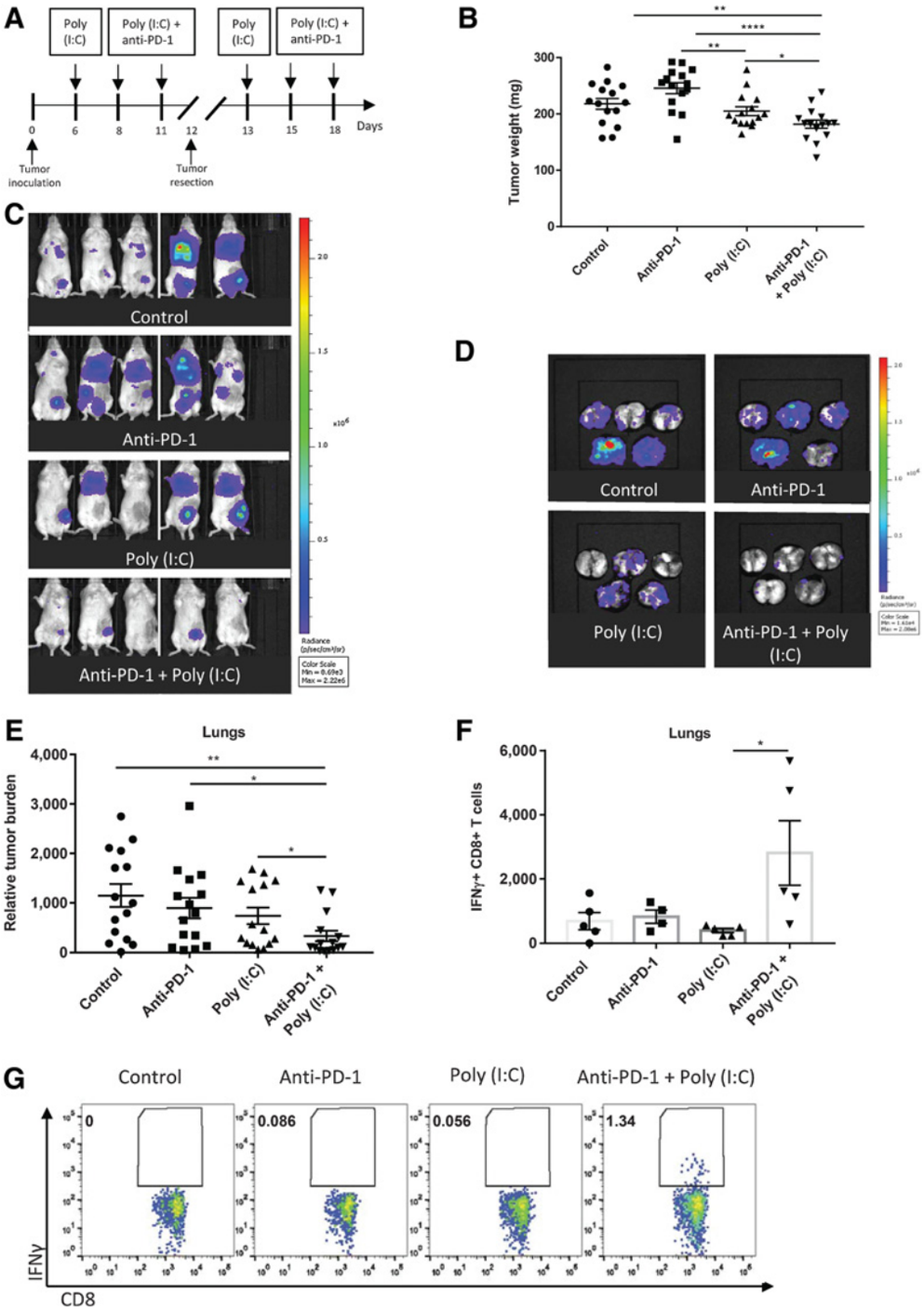

Figure 4.

Antibody-mediated blockade of the PD-1/PD-L1 axis in combination with poly(I:C) decreases primary tumor weight and increases systemic expansion of tumor-specific $CD8^+$ T cells. **A,** Treatment protocol for combination therapy of BALB/C mice inoculated IMFP with 1×10^5 4T1.2 cells and treated with poly(I:C) (25 μg, i.v.) and anti–PD-1 (RPM1-14; 250 μg, i.p.). **B,** Tumor weight (mg) 12 days after tumor cell inoculation ($n = 15$ per group). Bioluminescent imaging of (**C**) whole mice and (**D**) *ex vivo* lungs collected from 4T1.2 tumor–bearing mice 22 days after inoculation ($n = 5$ representative mice). **E,** Relative tumor burden (RTB) in lungs of mice represents mCherry DNA expression compared with vimentin ($n = 15$ per group). **F,** Single-cell suspensions of lung were restimulated *in vitro* with 4T1.2 cells in the presence of BFA (10 μg/mL). Following a five-minute incubation, $CD8^+$ T cells were assessed for IFNγ production via flow cytometry after staining with APC-conjugated anti-CD8α (53-6.7) and PE-conjugated anti-IFNγ (XMG1.2) in an ICS assay. Absolute numbers per lung shown, $n = 5$ per group. **G,** Representative flow-cytometry plots for IFNγ and CD8 staining. Representative of two independent mouse experiments. Error bars represent SEM; *, $P < 0.05$; **, $P < 0.01$; ***, $P < 0.001$; ****, $P < 0.0001$ using Student *t* tests.

Downloaded from http://aacrjournals.org/cancerimmunolres/article-pdf/5/10/871/2351462/871.pdf by guest on 26 August 2022

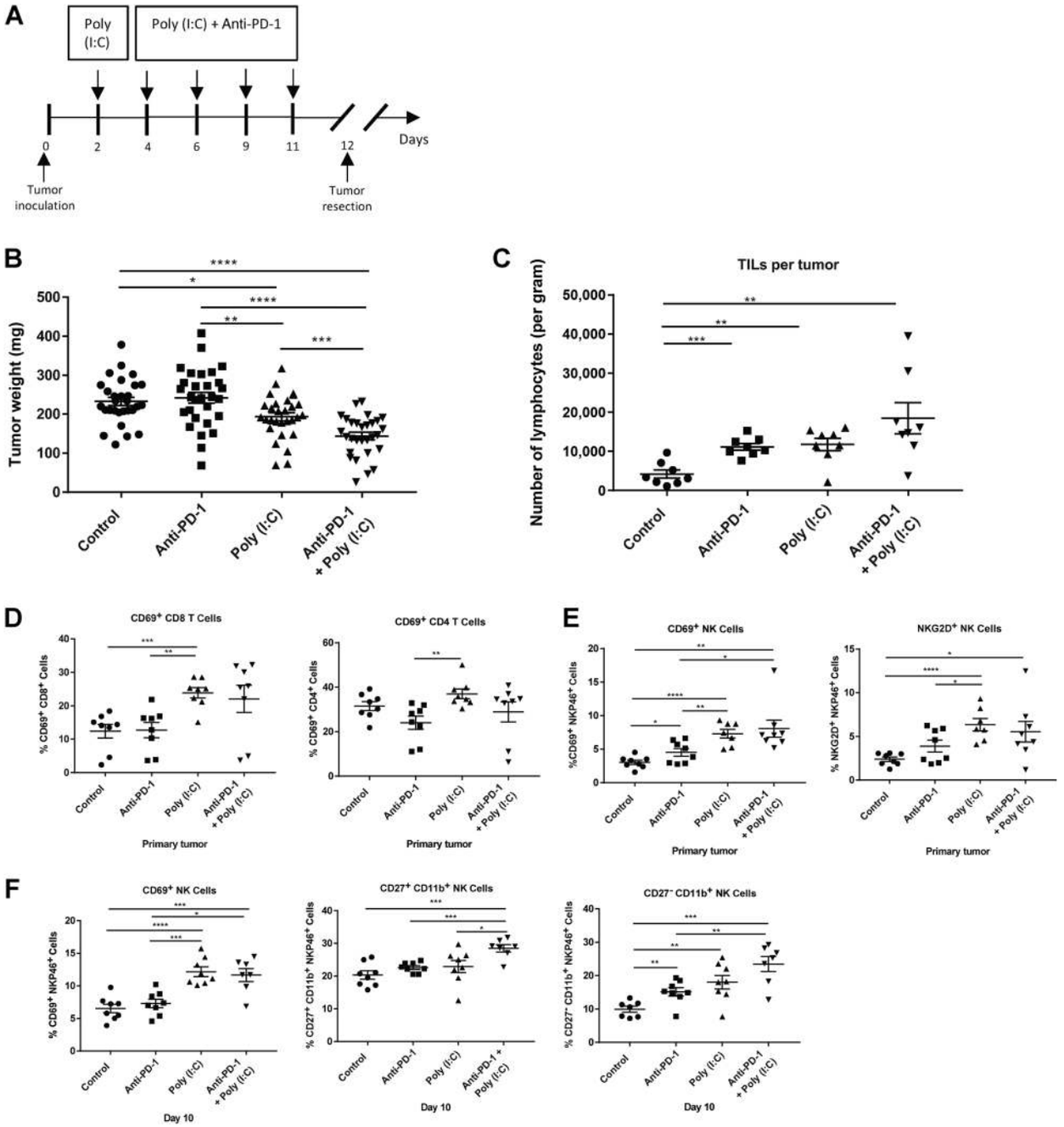

Figure 5.

Neoadjuvant poly(I:C) and combination therapy increases TIL activation. **A,** Treatment protocol for combination therapy of BALB/C mice injected with 1×10^5 4T1.2 cells IMFP and treated with poly(I:C) (25 μg, i.v.) and anti–PD-1 (RPM1-14; 250 μg, i.p.). **B,** Tumor weight (mg) 12 days after tumor cell inoculation ($n = 29$ per group; representative of 3 independent mouse experiments). **C,** Absolute number of lymphocytes obtained from the primary tumor per gram. Proportion of (**D**) $CD8^+$, $CD4^+$, and (**E**) $NKp46^+$lymphocytes expressing CD69/NKG2D isolated from the primary tumor at the time of resection (D12). **F,** Percentage of $NKp46^+$ lymphocytes expressing CD69/CD27/CD11b isolated from peripheral blood of 4T1.2 tumor–bearing BALB/C mice at day 10; $n = 8$ per group; error bars represent SEM; *, $P < 0.05$; **, $P < 0.01$; ***, $P < 0.001$ ****, $P < 0.0001$ using Student t test.

Discussion

This study highlights the antimetastatic effects of targeted type I IFN activation in multiple models of TNBC. Analysis of the interplay between IFNs and PD-L1 expression revealed the secondary upregulation of PD-L1 and PD-1 in response to enhanced immune activation and IFN production. Our *in vivo* analyses into coadministration of anti–PD-1 and poly(I:C) revealed that anti–PD-1 is ineffective as a stand-alone agent but

Downloaded from http://aacrjournals.org/cancerimmunolres/article-pdf/5/10/871/2351462/871.pdf by guest on 26 August 2022

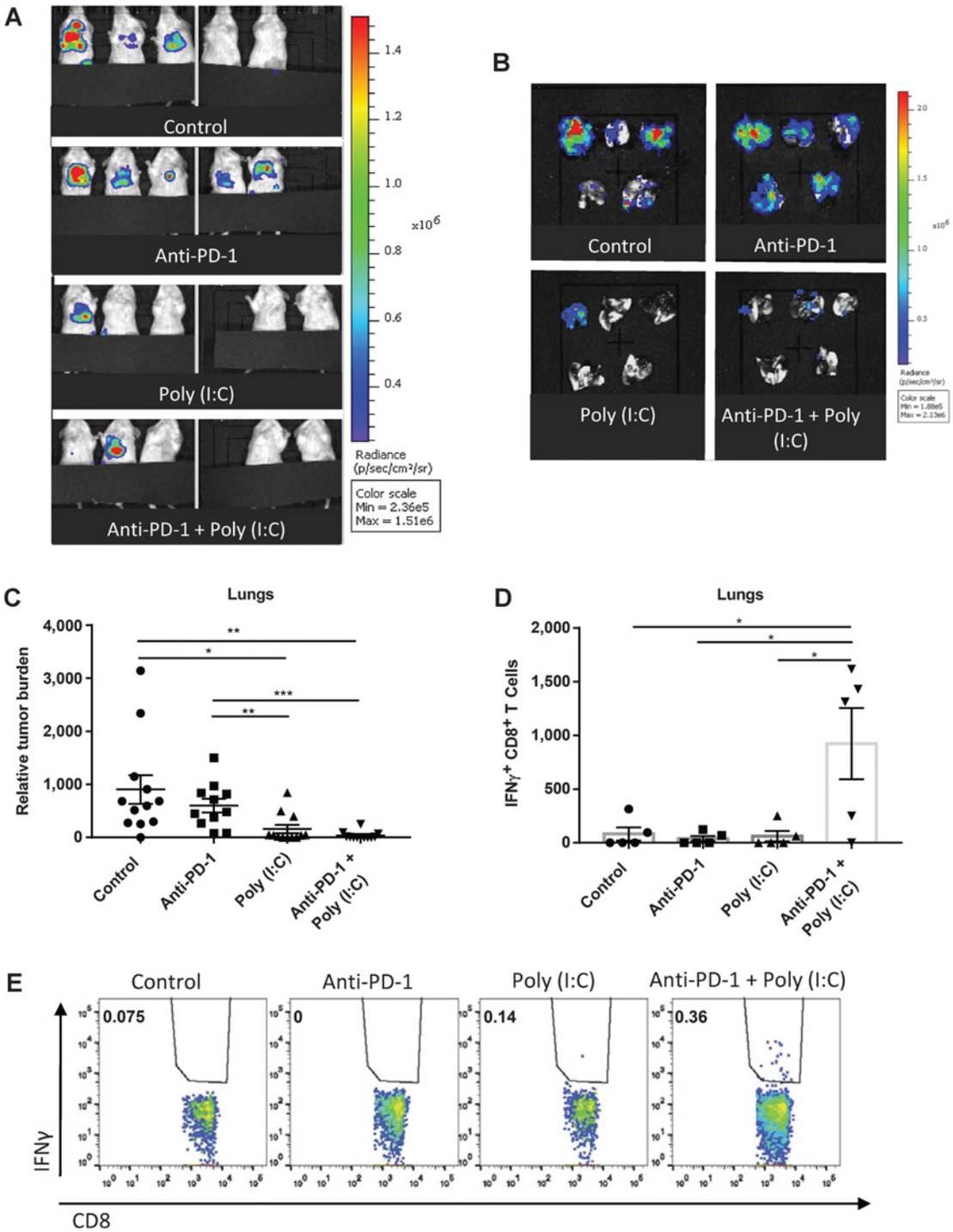

Figure 6.

Neoadjuvant poly(I:C) and combination therapy reduced metastatic burden. Bioluminescent imaging after D-Luciferin injection (1.5 mg, i.p.) of (**A**) whole mice and (**B**) *ex vivo* lungs collected from 4T1.2 tumor–bearing mice 23 days after tumor inoculation (of 5 mice representative of larger cohort; mice skirted during imaging to block any possible bioluminescence from the lower half to focus purely on thoracic cavity metastases). **C,** RTB in lungs represents mCherry tumor cell expression compared with Vimentin ($n = 12$ per group). **D,** Single-cell suspensions of lung were restimulated *in vitro* with 4T1.2 cells in the presence of BFA (10 μg/mL). Following a five-minute incubation, $CD8^+$ T cells were assessed for IFNγ production via flow cytometry after staining with APC-conjugated anti-CD8α (53-6.7) and PE-conjugated anti-IFNγ (XMG1.2) in an ICS assay. Absolute numbers per lung shown, $n = 5$ per group. **E,** Representative flow-cytometry plots for IFNγ and CD8 staining. Representative of two independent mouse experiments. Error bars represent SEM; *, $P < 0.05$; **, $P < 0.01$; ***, $P < 0.001$; ****, $P < 0.0001$ using Student *t* tests.

Downloaded from http://aacrjournals.org/cancerimmunolres/article-pdf/5/10/871/2351462/871.pdf by guest on 26 August 2022

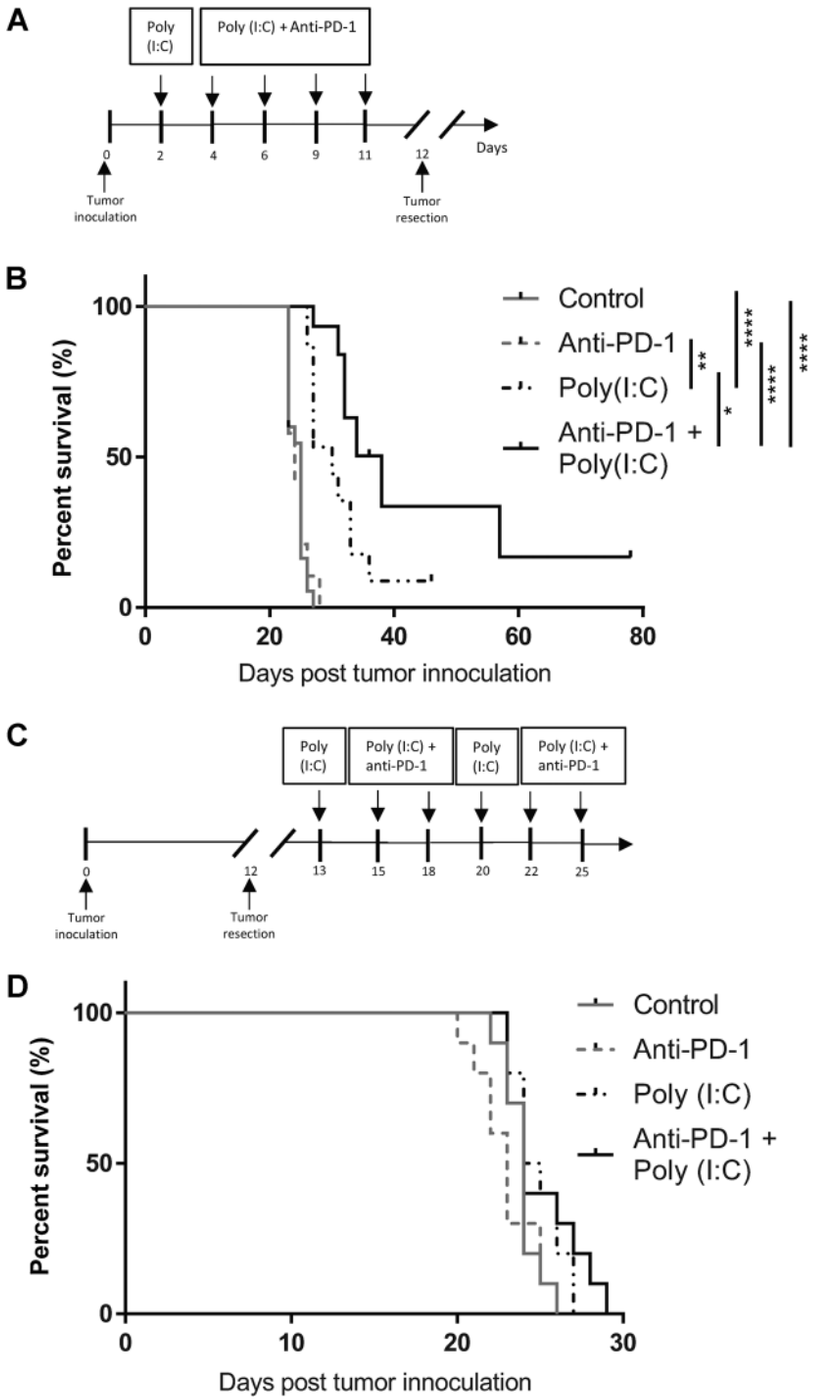

Figure 7.

Neoadjuvant poly(I:C) combined with anti–PD-1 therapy prolonged survival. **A** and **C,** Treatment protocol for combination therapy of BALB/C mice injected with 1×10^5 4T1.2 cells IMFP and treated with poly(I:C) (25 μg, i.v.) and anti–PD-1 (RPM1-14; 250 μg, i.p.). **B** and **D,** Kaplan–Meier survival curve comparing metastasis-free survival in mice treated with vehicle, poly(I:C), anti–PD-1 (RMP1-14), or the combination [$n = 15$ per group; representative of two independent mouse experiments (**B**), $n = 10$ per group (**D**)]. Mice excluded due to primary tumor regrowth are indicated. *, $P < 0.05$; **, $P < 0.01$; ****, $P < 0.0001$ using Student *t* test.

can prolong the antitumor T-cell response and therapeutic benefit of poly(I:C), specifically in the neoadjuvant setting.

Investigating the interplay between enhanced IFN signaling and PD-L1 expression confirmed PD-L1 as an IFN-regulated gene in TNBC. PD-L1 is a known ISG that is upregulated in response to immune activating cytokines in both tumor and tumor-associated stromal cells (40). We found that a key set of type I IFN genes, encompassing essential transcription factors, correlated with PD-L1 expression in TNBC, as described by other groups in primary and metastatic melanoma (41). Tumoral PD-L1 expression reflects an active antitumor microenvironment (42), offering support as to why PD-L1 is a good prognostic factor in TNBC (8, 9). PD-L1 expression correlates with the presence of TILs, and tumors that are rich in immune cells or "hot" have been associated with a better prognosis in both TNBC and melanoma (10, 43–45). We have also previously shown that retained tumor-intrinsic IFN in the primary tumor is associated with increased relapse-free survival in breast cancer (16).

Downloaded from http://aacrjournals.org/cancerimmunolres/article-pdf/5/10/871/2351462/871.pdf by guest on 26 August 2022

By using a treatment that directly enhances IFN signaling both in tumor and immune cells, we increased the intratumoral and microenvironmental immune activation in previously "immune cell poor" or "cold" tumors, which resulted in improved survival outcomes. As noted previously, there is a lack of utility of IFN-based treatments in breast cancer due to the inconsistent efficacy data in late metastatic treatment settings (14). Our data support the ineffectiveness of IFN-based treatments in the late metastatic treatment setting where poly(I:C) offered no survival benefit at all. This is in support of the continued success of IFN treatment in adjuvant high-risk melanoma, where it is used before overt metastases are present (20). Our study demonstrated that a neoadjuvant approach with poly(I:C) treatment was better for suppressing metastatic spread than later treatment settings. A benefit of a neoadjuvant approach rather than late-stage immunotherapy in TNBC has also been reported by others (46) and is consistent with previous breast cancer trials where poly (A:U) showed most promise in an early treatment setting (14). We hypothesize that a loss of intrinsic IFN signaling in the tumor may predict benefit from IFN-based therapies.

Clinical trials designed to test the efficacy of anti–PD-1/PD-L1 agents in breast cancer include patients have been based on the presence of tumoral PD-L1 expression. Our work, however, along with other work in breast and melanoma suggests that baseline PD-L1 expression is not a sufficiently sensitive predictor of response (6, 12). In a phase Ib clinical trial where TNBC patients were recruited based on PD-L1 positivity (>1%), the efficacy of pembroluzimab was underwhelming with a response rate of 18.5% (12). Another study suggested that anti–PD-1 was an effective single agent in a neoadjuvant TNBC mouse model (46). Our data, on the other hand, show a lack of efficacy of anti–PD-1 as a single agent in multiple models of TNBC. Others have similarly found a lack of response to anti–PD-1 in mouse models of TNBC (47). The lack of antimetastatic effect of anti–PD-1 reveals the inability of anti–PD-1 alone to induce an antitumor immune response. This demonstrates that a potent immune stimulator in addition to anti–PD-1 is required for an antimetastatic response. In line with a link between anti–PD-1 response and an active tumor-infiltrate, increased $CD8^+$, $CD3^+$, and $CD45RO^+$ T-cell densities at the invasive tumor margin correlate with response to anti–PD-1 in melanoma (48). Although we have shown that both anti–PD-1 and poly(I:C) alone and in combination increase intratumoral lymphocytes, our data demonstrate that it is the nature of such TILs that correlates with response to therapy. Anti–PD-1 treatment alone was not sufficient for TIL activation in our study, whereas combination with poly(I:C) enhanced both T-cell and NK-cell activation, essentially heating up a previously immune-inactive tumor to promote antitumor response and benefit from anti–PD-1 therapy. Melanoma studies support this proposition, whereby stimulation of IFN signaling and immune activation in immune cell poor melanomas is necessary for anti–PD-1 treatment to be effective (41).

Although poly(I:C) was an effective agent in the neoadjuvant setting in our study, we also demonstrate a therapeutic benefit with the addition of anti–PD-1. The increase in overall survival from the combination therapy in a neoadjuvant setting is likely due to the induction of a tumor specific T-cell response, which works to eliminate metastases. In the context of neoadjuvant therapy, the presence of the primary tumor *in situ* allows for the priming of tumor-specific cytotoxic T cells (46). The combination therapy, which was superior to single agents in overall survival, correlated with an increase in tumor-specific cytotoxic T cells at the site of metastasis. This finding suggests that the combination therapy induced a self-renewing residential memory population within metastases, as demonstrated by elevated $IFN\gamma^+$ $CD8^+$ T cells persisting in the lung up to 12 days after treatment cessation, which is after the T-cell contraction phase. Induction of a memory population is likely critical for a sustained antimetastatic therapeutic response given that breast cancer recurrence can occur years after initial diagnosis (49). The immune targeting of micrometastases before the formation of overt metastases would represent a major therapeutic advance in TNBC. Others have also shown that targeting multiple suppressive pathways is more effective than using single agents alone (2, 47, 50, 51). Here, we demonstrate that increasing immune activation through type I IFN stimulation can enhance the efficacy of anti–PD-1 in TNBC through induction of a tumor-specific immune response. Studies that have sought to increase tumor intrinsic interferon signaling alone or in combination with anti–PD-1 in other cancers have also had successes, particularly with treatments that can activate cytotoxic T cells and decrease immune suppressive populations (41, 52, 53).

In summary, we have demonstrated the ineffectiveness of anti–PD-1 as a single agent and the potential clinical use of combination type I IFN inducers and anti–PD-1 therapy in preclinical TNBC models. Our findings reveal that IFN signaling must be stimulated to promote immune activation in order for anti–PD-1 to be effective. These findings should be considered when designing clinical trials evaluating anti–PD-1 therapies in TNBC. Future research into tumor-intrinsic IFN markers as predictive biomarkers of response to IFN-based and anti–PD-1 therapies is needed. Our research suggests that patients with immune "cold" tumors can be primed to respond to anti–PD-1 therapy via type I IFN-based therapy, and that elevated tumor-cell expression of PD-L1 may serve as a biomarker for this therapeutic approach.

This study highlights the antimetastatic effects of targeted type I IFN activation in multiple models of TNBC. Analysis of the interplay between IFNs and PD-L1 expression revealed the secondary upregulation of PD-L1 and PD-1 in response to enhanced immune activation and IFN production. Our *in vivo* analyses into coadministration of anti–PD-1 and poly(I:C) revealed that anti–PD-1 is ineffective as a stand-alone treatment but can prolong the antitumor T-cell response and therapeutic benefit of poly(I:C) in the neoadjuvant setting. Given current clinical trials using TLR agonists in oncology (54), our combination therapy can be directly translated into the clinical setting.

Disclosure of Potential Conflicts of Interest

S. Loi reports receiving commercial research grants from Merck, Roche Genentech, Pfizer, and Bristol-Myers Squibb. E. Lim reports receiving commercial research grants from Novartis and Bayer. No potential conflicts of interest were disclosed by the other authors.

Authors' Contributions

Conception and design: E. Lim, B.S. Parker

Development of methodology: D. Zanker, E. Lim

Acquisition of data (provided animals, acquired and managed patients, provided facilities, etc.): N.K. Brockwell, K.L. Owen, D. Zanker, J. Rautela, E. Lim, B.S. Parker

Analysis and interpretation of data (e.g., statistical analysis, biostatistics, computational analysis): N.K. Brockwell, D. Zanker, F. Caramia, S. Loi, P.K. Darcy, E. Lim, B.S. Parker

Downloaded from http://aacrjournals.org/cancerimmunolres/article-pdf/5/10/871/2351462/871.pdf by guest on 26 August 2022

Writing, review, and/or revision of the manuscript: N.K. Brockwell, K.L. Owen, D. Zanker, H.M. Duivenvoorden, F. Caramia, S. Loi, P.K. Darcy, E. Lim, B.S. Parker
Administrative, technical, or material support (i.e., reporting or organizing data, constructing databases): D. Zanker, A. Spurling, H.M. Duivenvoorden, N. Baschuk
Study supervision: E. Lim, B.S. Parker

Acknowledgments

We acknowledge La Trobe Animal Research Training Facility (LARTF) for their support with animal work.

Grant Support

This work was supported by grant funding from the National Health and Medical Research Council (NHMRC, APP1047747) and Cancer Council Victoria (APP1127757; B.S. Parker). Fellowship support was received from NHMRC and ARC (P.K. Darcy and B.S. Parker) and the National Breast Cancer Foundation (fellowship to E. Lim).

The costs of publication of this article were defrayed in part by the payment of page charges. This article must therefore be hereby marked *advertisement* in accordance with 18 U.S.C. Section 1734 solely to indicate this fact.

Received March 27, 2017; revised July 8, 2017; accepted August 21, 2017; published OnlineFirst August 28, 2017.

References

1. Robert C, Thomas L, Bondarenko I, O'Day S, Weber J, Garbe C, et al. Ipilimumab plus dacarbazine for previously untreated metastatic melanoma. N Engl J Med 2011;364:2517–26.
2. Ott PA, Hodi FS, Robert C. CTLA-4 and PD-1/PD-L1 blockade: new immunotherapeutic modalities with durable clinical benefit in melanoma patients. Clin Cancer Res 2013;19:5300–9.
3. Kataoka K, Ogawa S. Novel mechanism of immune evasion involving PD-L1 in various cancers. Transl Cancer Res 2016;5:S428–S32.
4. Beatty GL, Gladney WL. Immune escape mechanisms as a guide for cancer immunotherapy. Clin Cancer Res 2015;21:687–92.
5. Robert C, Long GV, Brady B, Dutriaux C, Maio M, Mortier L, et al. Nivolumab in previously untreated melanoma without BRAF mutation. N Engl J Med 2015;372:320–30.
6. Robert C, Schachter J, Long GV, Arance A, Grob JJ, Mortier L, et al. Pembrolizumab versus ipilimumab in advanced melanoma. N Engl J Med 2015;372:2521–32.
7. Hodi FS, Kluger H, Sznol M, Carvajal R, Lawrence D, Atkins M, et al. Abstract CT001: Durable, long-term survival in previously treated patients with advanced melanoma (MEL) who received nivolumab (NIVO) monotherapy in a phase I trial. Cancer Res 2016;76: no. 14 Supplement, CT001–CT001.
8. Beckers RK, Selinger CI, Vilain R, Madore J, Wilmott JS, Harvey K, et al. Programmed death ligand 1 expression in triple-negative breast cancer is associated with tumour-infiltrating lymphocytes and improved outcome. Histopathology 2016;69:25–34.
9. Sabatier R, Finetti P, Mamessier E, Adelaide J, Chaffanet M, Ali HR, et al. Prognostic and predictive value of PDL1 expression in breast cancer. Oncotarget 2015;7:5449–69.
10. Wimberly H, Brown JR, Schalper KA, Haack H, Silver MR, Nixon C, et al. PD-L1 expression correlates with tumor-infiltrating lymphocytes and response to neoadjuvant chemotherapy in breast cancer. Cancer Immunol Res 2015;3:326–32.
11. Miller LD, Chou JA, Black MA, Print C, Chifman J, Alistar A, et al. Immunogenic subtypes of breast cancer delineated by gene classifiers of immune responsiveness. Cancer Immunol Res 2016;4:600–10.
12. Nanda R, Chow LQM, Dees EC, Berger R, Gupta S, Geva R, et al. Pembrolizumab in patients with advanced triple-negative breast cancer: Phase Ib KEYNOTE-012 Study. J Clin Oncol 2016;34:2460–7.
13. Ali HR, Provenzano E, Dawson SJ, Blows FM, Liu B, Shah M, et al. Association between CD8+ T-cell infiltration and breast cancer survival in 12,439 patients. Ann Oncol 2014;25:1536–43.
14. Parker BS, Rautela J, Hertzog PJ. Antitumour actions of interferons: implications for cancer therapy. Nat Rev Cancer 2016;16:131–44.
15. Swann JB, Hayakawa Y, Zerafa N, Sheehan KC, Scott B, Schreiber RD, et al. Type I IFN contributes to NK cell homeostasis, activation, and antitumor function. J Immunol 2007;178:7540–9.
16. Bidwell BN, Slaney CY, Withana NP, Forster S, Cao Y, Loi S, et al. Silencing of Irf7 pathways in breast cancer cells promotes bone metastasis through immune escape. Nat Med 2012;18:1224–31.
17. Rautela J, Baschuk N, Slaney CY, Jayatilleke KM, Xiao K, Bidwell BN, et al. Loss of host type-I IFN signaling accelerates metastasis and impairs NK-cell antitumor function in multiple models of breast cancer. Cancer Immunol Res 2015;3:1207–17.
18. Katlinskaya YV, Katlinski KV, Yu Q, Ortiz A, Beiting DP, Brice A, et al. Suppression of type I interferon signaling overcomes oncogene-induced senescence and mediates melanoma development and progression. Cell Rep 2016;15:171–80.
19. Di Trolio R, Simeone E, Di Lorenzo G, Buonerba C, Ascierto PA. The use of interferon in melanoma patients: a systematic review. Cytokine Growth Factor Rev 2015;26:203–12.
20. Ascierto PA, Gogas HJ, Grob JJ, Algarra SM, Mohr P, Hansson J, et al. Adjuvant interferon alfa in malignant melanoma: an interdisciplinary and multinational expert review. Crit Rev Oncol Hematol 2013;85:149–61.
21. Lacour J, Lacour F, Spira A, Michelson M, Petit JY, Delage G, et al. Adjuvant treatment with polyadenylic-polyuridylic acid in operable breast cancer: updated results of a randomised trial. Br Med J (Clin. Res. Ed). 1984; 288:589–92.
22. Laplanche A, Alzieu L, Delozier T, Berlie J, Veyret C, Fargeot P, et al. Polyadenylic-polyuridylic acid plus locoregional radiotherapy versus chemotherapy with CMF in operable breast cancer: a 14 year follow-up analysis of a randomized trial of the Federation Nationale des Centres de Lutte contre le Cancer (FNCLCC). Breast Cancer Res Treat 2000;64:189–91.
23. Dunn GP, Bruce AT, Sheehan KC, Shankaran V, Uppaluri R, Bui JD, et al. A critical function for type I interferons in cancer immunoediting. Nat Immunol 2005;6:722–9.
24. Zitvogel L, Galluzzi L, Kepp O, Smyth MJ, Kroemer G. Type I interferons in anticancer immunity. Nat Rev Immunol 2015;15:405–14.
25. Brinkmann V, Geiger T, Alkan S, Heusser CH. Interferon alpha increases the frequency of interferon gamma-producing human CD4+ T cells. J Exp Med 1993;178:1655–63.
26. Nguyen KB, Cousens LP, Doughty LA, Pien GC, Durbin JE, Biron CA. Interferon alpha/beta-mediated inhibition and promotion of interferon gamma: STAT1 resolves a paradox. Nat Immunol 2000;1:70–6.
27. Lee SJ, Jang BC, Lee SW, Yang YI, Suh SI, Park YM, et al. Interferon regulatory factor-1 is prerequisite to the constitutive expression and IFN-gamma-induced upregulation of B7-H1 (CD274). FEBS Lett 2006;580:755–62.
28. Riella LV, Paterson AM, Sharpe AH, Chandraker A. Role of the PD-1 pathway in the immune response. Am J Trans 2012;12:2575–87.
29. Aslakson CJ, Miller FR. Selective events in the metastatic process defined by analysis of the sequential dissemination of subpopulations of a mouse mammary tumor. Cancer Res 1992;52:1399–405.
30. Eckhardt BL, Parker BS, van Laar RK, Restall CM, Natoli AL, Tavaria MD, et al. Genomic analysis of a spontaneous model of breast cancer metastasis to bone reveals a role for the extracellular matrix. Mol Cancer Res 2005;3: 1–13.
31. Lelekakis M, Moseley JM, Martin TJ, Hards D, Williams E, Ho P, et al. A novel orthotopic model of breast cancer metastasis to bone. Clin Exp Metastasis 1999;17:163–70.
32. Casey AE, Laster WR, Ross GL. Sustained enhanced growth of carcinoma EO771 in C57 black mice. Exp Biol Med 1951;77:358–62.
33. Zanker D, Waithman J, Yewdell JW, Chen W. Mixed proteasomes function to increase viral peptide diversity and broaden antiviral CD8+T cell responses. J Immunol 2013;191:52–9.
34. Broad Institute TCGA Genome Data Analysis Center. Analysis-ready standardized TCGA data from Broad GDAC Firehose 2016_01_28 run. Broad Institute of MIT and Harvard. 2016.
35. Touati N, Tryfonidis K, Caramia F, Bonnefoi H, Cameron D, Slaets L, et al. Correlation between severe infection and breast cancer metastases in the EORTC 10994/BIG 1-00 trial: Investigating innate immunity as a tumor suppressor in breast cancer. Ann Oncol 2016;27:suppl_6, 256P–256P.

Downloaded from http://aacrjournals.org/cancerimmunolres/article-pdf/5/10/871/2351462/871.pdf by guest on 26 August 2022

36. Eckhardt BL, Francis PA, Parker BS, Anderson RL. Strategies for the discovery and development of therapies for metastatic breast cancer. Nat Rev Drug Discov 2012;11:479–97.
37. Soliman H, Khalil F, Antonia S. PD-L1 expression is increased in a subset of basal type breast cancer cells. PLoS One 2014;9:e88557.
38. Fu B, Wang F, Sun R, Ling B, Tian Z, Wei H. CD11b and CD27 reflect distinct population and functional specialization in human natural killer cells. Immunology 2011;133:350–9.
39. Seder RA, Ahmed R. Similarities and differences in CD4+ and CD8+ effector and memory T cell generation. Nat Immunol 2003;4:835–42.
40. Cheon H, Borden EC, Stark GR. Interferons and their stimulated genes in the tumor microenvironment. Semin Oncol 2014;41:156–73.
41. Bald T, Landsberg J, Lopez-Ramos D, Renn M, Glodde N, Jansen P, et al. Immune cell-poor melanomas benefit from PD-1 blockade after targeted type I IFN activation. Cancer Discov 2014;4:674–87.
42. Taube JM, Klein A, Brahmer JR, Xu H, Pan X, Kim JH, et al. Association of PD-1, PD-1 ligands, and other features of the tumor immune microenvironment with response to anti–PD-1 therapy. Clin Caner Res 2014;20:5064–74.
43. Adams S, Gray RJ, Demaria S, Goldstein L, Perez EA, Shulman LN, et al. Prognostic value of tumor-infiltrating lymphocytes in triple-negative breast cancers from two phase III randomized adjuvant breast cancer trials: ECOG 2197 and ECOG 1199. J Clin Oncol 2014;32:2959–66.
44. Salgado R, Denkert C, Demaria S, Sirtaine N, Klauschen F, Pruneri G, et al. The evaluation of tumor-infiltrating lymphocytes (TILs) in breast cancer: recommendations by an International TILs Working Group 2014. Ann Oncol 2015;26:259–71.
45. Oble DA, Loewe R, Yu P, Mihm MC. Focus on TILs: prognostic significance of tumor infiltrating lymphocytes in human melanoma. Cancer Immun 2009;9:3.
46. Liu J, Blake SJ, Yong MCR, Harjunpää H, Ngiow SF, Takeda K, et al. Improved efficacy of neoadjuvant compared to adjuvant immunotherapy to eradicate metastatic disease. Cancer Discov 2016;6:1382–99.
47. Beavis PA, Milenkovski N, Henderson MA, John LB, Allard B, Loi S, et al. Adenosine receptor 2A blockade increases the efficacy of anti-PD-1 through enhanced antitumor T-cell responses. Cancer Immunol Res 2015;3:506–17.
48. Gibney GT, Weiner LM, Atkins MB. Predictive biomarkers for checkpoint inhibitor-based immunotherapy. Lancet Oncol 2017;17:e542–51.
49. Banys M, Hartkopf AD, Krawczyk N, Kaiser T, Meier-Stiegen F, Fehm T, et al. Dormancy in breast cancer. Breast Cancer (London). 2012;4:183–91.
50. Callahan MK, Postow MA, Wolchok JD. CTLA-4 and PD-1 pathway blockade: combinations in the clinic. Front Oncol 2014;4:385.
51. Rajani K, Parrish C, Kottke T, Thompson J, Zaidi S, Ilett L, et al. Combination therapy with reovirus and anti-PD-1 blockade controls tumor growth through innate and adaptive immune responses. Mol Ther 2016;24:166–74.
52. Mkrtichyan M, Chong N, Abu Eid R, Wallecha A, Singh R, Rothman J, et al. Anti-PD-1 antibody significantly increases therapeutic efficacy of Listeria monocytogenes (Lm)-LLO immunotherapy. J Immunother Cancer 2013;1:15.
53. Katlinski KV, Gui J, Katlinskaya YV, Ortiz A, Chakraborty R, Bhattacharya S, et al. Inactivation of interferon receptor promotes the establishment of immune privileged tumor microenvironment. Cancer Cell 2017;31:194–207.
54. Iribarren K, Bloy N, Buqué A, Cremer I, Eggermont A, Fridman WH, et al. Trial Watch: Immunostimulation with Toll-like receptor agonists in cancer therapy. Oncoimmunology 2016;5:e1088631.

Downloaded from http://aacrjournals.org/cancerimmunolres/article-pdf/5/10/871/2351462/871.pdf by guest on 26 August 2022